Comparison of drift velocities of nighttime equatorial plasma depletions with ambient plasma drifts and thermospheric neutral winds

Guiping Liu,[1] Scott L. England,[1] Harald U. Frey,[1] Thomas J. Immel,[1] Chin S. Lin,[2] Edgardo E. Pacheco,[3] Kathrin Häusler,[4] and Eelco Doornbos[5]

Received 15 August 2013; revised 22 October 2013; accepted 24 October 2013; published 13 November 2013.

[1] This is the first study to compare plasma depletion drifts with the ambient plasma drifts and neutral winds in the post sunset equatorial ionosphere using global-scale satellite observations. The local time and latitude variations of the drift velocities of O^+ plasma depletions at 350–400 km altitude are derived from the observations of the far ultraviolet imager operated on the IMAGE satellite during 10 March to 7 June 2002. These depletion drift velocities are compared with the simultaneously measured ion drift velocities and neutral winds by the ROCSAT-1 and the CHAMP satellites for a similar time period. The analysis shows that the zonal drift velocity of plasma depletions is smaller than both the ambient ion zonal drift velocity and the neutral zonal wind at 18:00–20:00 magnetic local time, and after 21:00, the variations of these velocities are similar. The difference of the plasma depletion drift with the background is found to be smaller at lower latitudes. Furthermore, the zonal drift velocity of the depletion is found to have a large latitudinal gradient specifically at 12°–18° magnetic latitude, which again does not match the ambient ion drift and the neutral wind. This latitudinal difference has been reported by previous studies, but those studies use models and they only compare the depletion drifts with the modeled neutral winds. This study provides a measure of the difference that has never been studied before by any study using global observations. It has been suggested that polarization electric fields inside the plasma depletion structure drive the plasma to drift westward and thus the depletion structure moves to the east. The latitudinal gradient of the depletion drift velocity seen here in this study could also be explained by the polarization electric fields. For the C-shaped (reversed C) depletion, the polarization electric fields inside the depletion drive a westward drift of plasma and this drift velocity changes with increasing latitude. Consequently, the depletion drift has a latitudinal gradient becoming significant at higher latitudes.

Citation: Liu, G., S. L. England, H. U. Frey, T. J. Immel, C. S. Lin, E. E. Pacheco, K. Häusler, and E. Doornbos (2013), Comparison of drift velocities of nighttime equatorial plasma depletions with ambient plasma drifts and thermospheric neutral winds, *J. Geophys. Res. Space Physics*, *118*, 7360–7368, doi:10.1002/2013JA019329.

1. Introduction

[2] Large-scale plasma density depletions in the nighttime equatorial *F* region ionosphere are typically associated with equatorial spread *F* (ESF) [e.g., *Kelley et al.*, 1981]. The depletions generally align with geomagnetic field lines and the depletion regions extend to several thousands of kilometers in latitude but a few hundred kilometers in longitude [e.g., *Tsunoda et al.*, 1982]. Because the plasma density inside the depleted regions can be many times lower than the ambient plasma density [e.g., *Tsunoda et al.*, 1982; *Kil and Heelis*, 1998], the depletion structures are often referred to as plasma bubbles. The sharp density gradients at the edges of the depletion structures produce small-scale plasma irregularities that are believed to cause disruptions in transionospheric radio signals in communication and navigation system [*Basu et al.*, 2002]. Plasma bubbles have thus become an important research topic for many investigations.

[3] Mechanism of the generation of plasma bubbles has been investigated through both observational and modeling investigations [e.g., *Kelley et al.*, 1981; *Huang and Kelley*,

Additional supporting information may be found in the online version of this article.

[1]Space Sciences Laboratory, University of California Berkeley, Berkeley, California, USA.
[2]Air Force Research Laboratory, Kirtland AFB, New Mexico, USA.
[3]Institute for Scientific Research, Boston College, Newton, Massachusetts, USA.
[4]High Altitude Observatory, National Center for Atmospheric Research, Boulder, Colorado, USA.
[5]Delft University of Technology, Delft, The Netherlands.

Corresponding author: G. Liu, Space Sciences Laboratory, University of California, Berkeley, CA 94720, USA. (guiping@ssl.berkeley.edu)

2169-9380/13/10.1002/2013JA019329

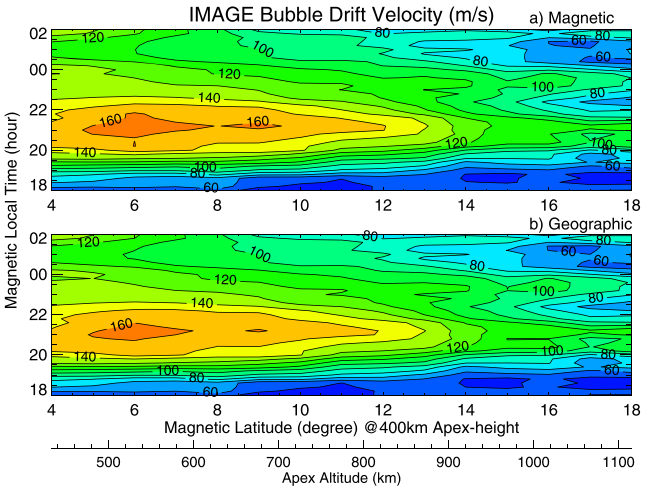

Figure 1. Zonally averaged mean values of plasma depletion drift velocities at 350–400 km altitude as derived from the IMAGE-FUV observations during 10 March to 7 June 2002 for (a) the magnetic zonal component and (b) the geographic zonal component. These drift velocities are presented versus magnetic latitude (MLAT) and magnetic local time (MLT). Corresponding apex altitudes of the observed MLATs are given at the bottom of the figure.

1996; *Fejer et al.*, 1999; *Makela*, 2006; *Huba et al.*, 2008; *Retterer*, 2010]. It is known that plasma depletions are excited in the bottom side *F* region and they grow higher up into the topside *F* region through the generalized Rayleigh-Taylor instability. The occurrence of plasma depletions depends on local time, and their global distribution changes with longitude, season, solar cycle, and magnetic activity [e.g., *Kil and Heelis*, 1998; *Fejer et al.*, 1999; *Su et al.*, 2009; *Huang et al.*, 2013].

[4] Plasma depletions are observed to drift in the zonal direction [e.g., *Abdu et al.*, 1985; *Fejer et al.*, 1991; *Valladares et al.*, 1996], and the depletions generally drift eastward [e.g., *Fejer et al.*, 1991; *Immel et al.*, 2003; *Lin et al.*, 2005; *Huang et al.*, 2010]. Using the C/NOFS satellite measurements, *Huang et al.* [2010] performed a survey of the relative zonal drift velocities of plasma inside the depletions with respect to the ambient plasma for many cases. They have found that for most cases, the relative plasma drift velocity inside the depletion structure is westward arising from polarization electric fields. The polarization electric fields drive the plasma inside the depletion to drift westward, and thus, the depletion structure moves to the east.

[5] The drift velocities of plasma depletions have also been found to relate with the background neutral winds [e.g., *Chapagain et al.*, 2012, 2013]. Because the *F* region dynamo dominates the nighttime plasma drifts [e.g., *Coley and Heelis*, 1989; *Heelis*, 2004], the ionized plasma at *F* region altitudes moves eastward at approximately the same speed as the neutral atmosphere. The O I 630.0 nm airglow emission observations allow for the depletion drift velocities and the neutral winds in the thermosphere to be simultaneously measured [*Makela*, 2006]. Direct comparison has shown that the depletion drift velocities are approximately equal to the background wind speeds at nighttime hours after 22:00 LT and the depletion drifts are slower at 18:00–20:00 LT as the *E* region is still present [*Chapagain et al.*, 2012, 2013].

[6] Furthermore, the zonal drift velocities of plasma depletions have a latitudinal gradient, the result of which is a westward tilt of the depletion structures with increasing latitude [e.g., *Mendillo and Tyler*, 1983]. The structures appear as a reversed C shape when viewed across both hemispheres [e.g., *Kelley et al.*, 1981]. The C-shaped plasma structures have been attributed to the effects of the *F* region neutral wind [*Anderson and Mendillo*, 1983; *Haase et al.*, 2011] and/or the ionospheric Pederson conductivity [*Zalesak et al.*, 1982; *Martinis et al.*, 2003]. Including the HWM93 wind model, the SAMI3/ESF model reproduces a reversed C-shaped plasma depletion as the observations [*Huba et al.*, 2009]. The simulations demonstrate that the HWM93 wind model results agree better with the observations than those from a constant wind model.

[7] The space-based IMAGE-far ultraviolet (FUV) instrument at high-altitude orbits provided global-scale observations of plasma depletions, specifically allowing for the motion of the depletions to be tracked [e.g., *Immel et al.*, 2003; *Lin et al.*, 2005; *Park et al.*, 2007]. Using the IMAGE-FUV observations, *England and Immel* [2012] were able to build a large database of the zonal drift velocities of plasma depletions across the globe. This database has illustrated that the drift velocities of plasma depletions vary with latitude and local time. *England and Immel* [2012] have found that for the zonal drift velocities, the local time variations of the plasma depletions are similar to the background neutral winds as modeled by an empirical and a first-principles model but the plasma depletions have a larger latitudinal gradient. They have proposed that the difference in latitudinal gradient between the depletion drift velocities and the background neutral winds could be caused by polarization electric fields inside the depletions.

[8] For this study, we use the same database of the zonal drift velocities of plasma depletions built upon the

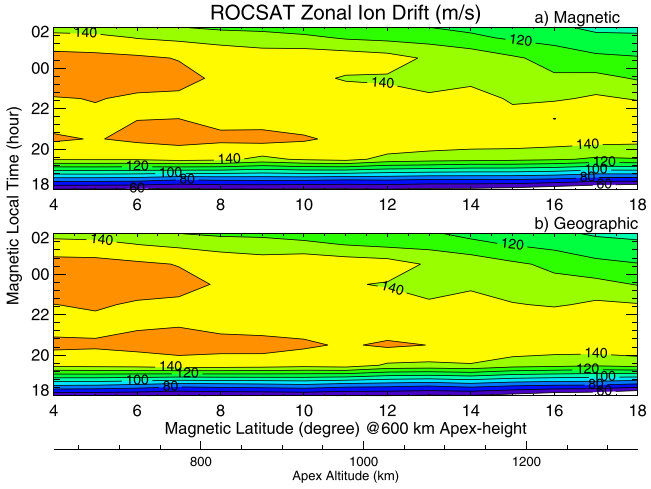

Figure 2. Zonally averaged mean values of ion drift velocities at ∼600 km altitude as measured by ROCSAT-1 throughout 10 March to 9 June 2002 for (a) the magnetic zonal component and (b) the geographic zonal component. Apex altitudes of the observed MLATs are given at the bottom of the figure.

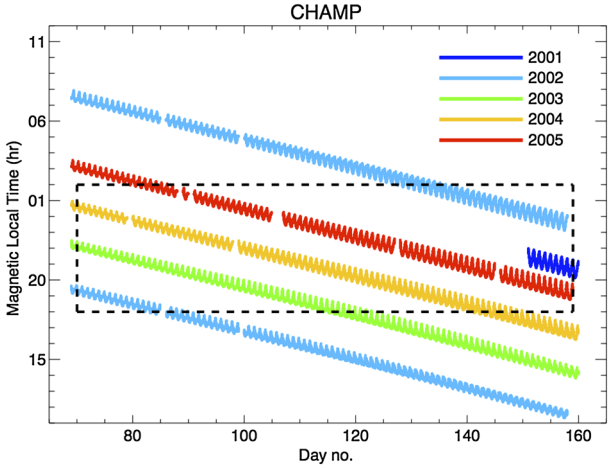

Figure 3. Sampling of the CHAMP satellite observations during 10 March to 9 June (day number 69–160) for 2001–2005. The MLTs of the observations in each day are given. Data are plotted in different colors for different years. The dashed lines outline the range of the data used for this study.

IMAGE-FUV observations. We directly compare these depletion drift velocities with the ambient ion drift velocities as well as the thermospheric neutral winds measured by the ROCSAT-1 and the CHAMP satellites during the similar time period. The previous studies by *Huba et al.* [2009] and *England and Immel* [2012] use models, and they only compare the depletion drifts with the modeled neutral winds. This study compares the satellite observations for global scales, and the study compares the depletion drifts with both the neutral winds and the plasma drifts using the observations. These observations provide a more reliable comparison than the models and thus allow more definitive conclusions to be drawn. We have performed the comparison for a range of local times and latitudes, and we seek to gain a better understanding of the variations of the depletion drift velocities with local time and latitude.

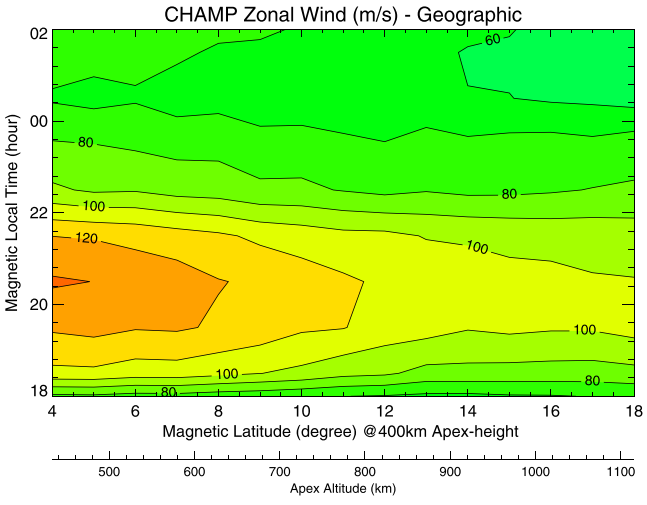

Figure 4. Zonally averaged mean values of geographic zonal winds from the CHAMP measurements at ~400 km altitude in the thermosphere during 10 March to 9 June of 2001-2005. Apex altitudes of the observed MLATs are given at the bottom of the figure.

2. Observations

2.1. Plasma Depletion Zonal Drift Velocities

[9] The far ultraviolet (FUV) imager operated on the IMAGE satellite observed the 135.6 nm O^+ airglow emission that peaks at 350–400 km. The spacecraft was launched in March 2000 into a highly elliptical orbit with the apogee altitudes of 7.2 R_E. During the Northern Hemisphere spring of 2002, the satellite apogee was in the evening sector and the FUV was able to continuously observe the post sunset equatorial airglow arc for several hours. The O^+ emission is bright during 2002 due to the large solar extreme ultraviolet flux. This allows for reliable identifications of plasma depletions in the IMAGE-FUV O^+ airglow emission observations over this time period.

[10] *Park et al.* [2007] and *England and Immel* [2012] have described the image analysis technique for Tracking of Airglow Depletions (TOAD) using the IMAGE-FUV airglow observations. The TOAD analysis creates a database for the 2002 Northern Hemisphere spring, including more than 200 plasma depletions and their moving tracks throughout several consecutive hours from the sunset to the early morning. This database allows for calculations of the drift velocities of plasma depletions in the magnetic zonal direction.

[11] Figure 1a presents the zonally averaged mean values of the zonal drift velocities of plasma depletions calculated using the IMAGE-FUV database for the time period of 10 March to 7 June 2002. The calculated depletion drift velocities are binned at 1° magnetic latitude (MLAT) and 12 min magnetic local time (MLT) intervals. As the plasma depletions are magnetic conjugate, the data in the two hemispheres are combined. The IMAGE-FUV database does not contain sufficient samples to also sort the data by magnetic longitude, so the results shown represent the magnetic zonal means. The uncertainties are large for the calculations at the equator and at high latitudes, where the O^+ emission is dim, so the drift velocities are presented for latitudes between 4° and 18°.

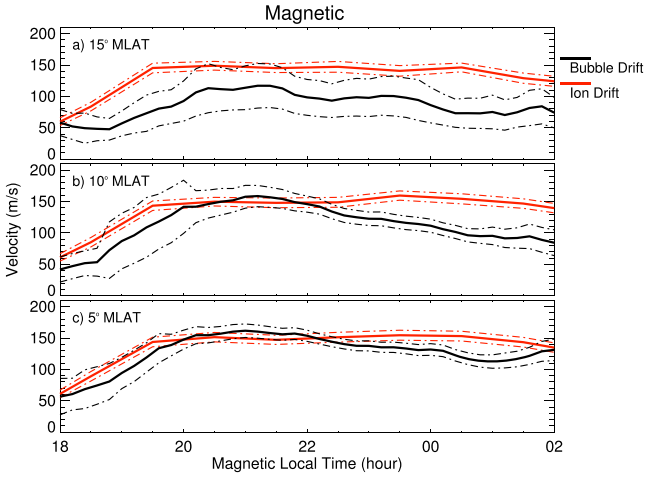

Figure 5. (a–c) Magnetic zonal velocities of plasma depletion drifts (in black) and ion drifts (in red) at various MLATs, presented versus MLTs. The dash-dotted lines represent 1 standard deviation of the velocities.

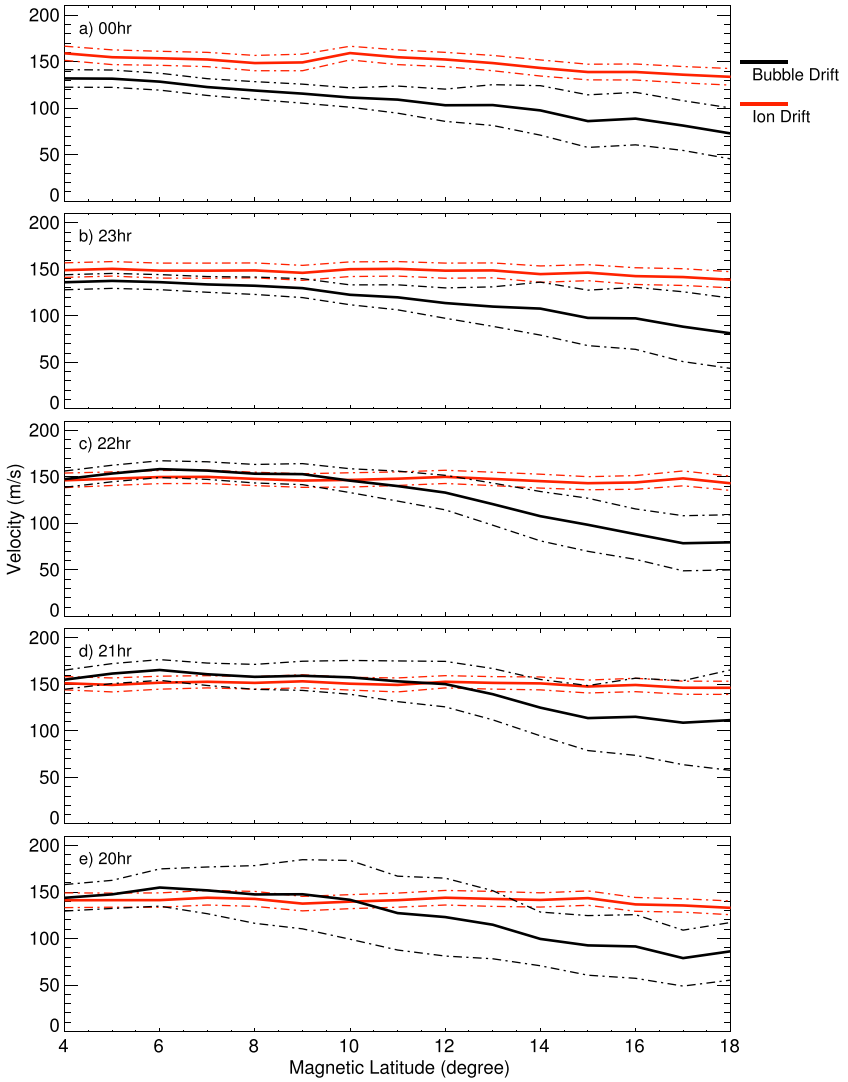

Figure 6. (a–e) Magnetic zonal velocities of plasma depletion drifts (in black) and ion drifts (in red) at various MLTs, presented versus MLAT. The dash-dotted lines represent 1 standard deviation of the velocities.

[12] As shown in Figure 1a, the zonal drift velocities of plasma depletions are all positive values, showing an eastward motion. The drift velocity changes with MLAT and MLT, being the largest at low latitudes at ~21:00 MLT. The velocity is smaller at higher latitudes, and the value decreases at post sunset and after 22:00 MLT. The plasma depletion drift velocities have already been presented in terms of meter(s) per second (m/s) and degrees/hour by *England and Immel* [2012]. The overall patterns are similar between them, so the change of the magnetic field geometry with MLAT is not responsible for the features discussed here. For this study, we present the depletion drift velocities in terms of m/s, and we include the observations at all longitudes and in the magnetic conjugate hemispheres.

2.2. Ion Zonal Drift Velocities

[13] The ROCSAT-1 satellite operated in a low-Earth near-spherical orbit at ~600 km altitude with 35° inclination during March 1999 to June 2004 [e.g., *Su et al.*, 2001]. The onboard Ionospheric Plasma and Electrodynamics Instrument measured in situ ion densities and three perpendicular components of ion drift velocities in the spacecraft frame at 1 s cadence with a 100% duty cycle. The ROCSAT-1 satellite provided critical measurements of the ion properties in the *F* region ionosphere.

[14] This study uses the ion drift velocity measurements taken by ROCSAT-1 during the same time period as the IMAGE-FUV plasma depletion observations throughout 10 March to 9 June 2002. The offsets of these measurements have been removed for three ion drift components, assuming a constant value in each component over this March–June time period. Methods for identifying the ROCSAT-1 measurement offsets have been described [e.g, *Pacheco et al.*, 2010]. We have also removed spikes and applied a 10 data point running average to the measurements. Finally, the three components of ion velocity measured in the spacecraft frame are transformed into the field-aligned (parallel) component and the two perpendicular components in the magnetic coordinate system using the International Geomagnetic Reference Field magnetic field model. The parallel component is

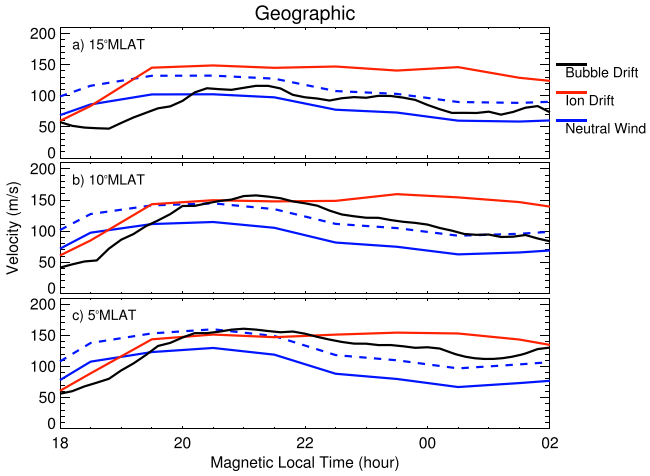

Figure 7. (a–c) Geographic zonal velocities of plasma depletion drifts (in black), ion drifts (in red), and neutral winds (in blue) at various MLATs, presented versus MLT. The solid blue lines are for the measured neutral winds by CHAMP, and the dashed blue lines are for the adjusted neutral winds using the HWM93 model.

along the magnetic field direction. One perpendicular component is chosen to be perpendicular to the magnetic field on the meridional plane (in the outward/upward directions). The other velocity component is perpendicular to both the magnetic field and the outward/upward directions, and it is in the magnetic zonal (eastward) direction.

[15] Figure 2a gives the zonal velocities of ion drifts in magnetic coordinates. The velocities in the magnetic conjugate hemispheres are binned for MLAT and MLT. These velocities exclude the values when plasma depletions are present. Plasma depletions have been identified in this study using the same method as described by *Su et al.* [2006] and *Kil and Heelis* [1998]. The figure thus includes the ambient ion drift velocities surrounding the plasma depletions.

[16] Figure 2a shows that the ion drift velocities have two maximums at low latitudes at around 21:00 MLT and midnight. The velocity is smaller at post sunset and during the post midnight hours and at higher latitudes. Compared to the plasma depletion drifts (see Figure 1), the ion drift velocity has one maximum occurring at similar MLTs and MLATs. There are also differences between the plasma depletion drifts and the ambient ion drifts, which are discussed in section 3.

2.3. Thermospheric Zonal Winds

[17] The CHAMP satellite was launched in July 2000 into a ∼450 km altitude orbit with inclination of 87.2°. Cross-track winds have been derived from the highly accurate measurements of the onboard triaxial accelerometer [e.g., *Doornbos et al.*, 2010; *Lieberman et al.*, 2013]. Due to the high inclination of the satellite, the cross-track winds obtained at latitudes less than 75° are almost entirely zonal (positive in eastward). The satellite reentered the atmosphere in 2010, and the thermospheric neutral wind data are available until the end of August 2010. For this study, the zonal winds from CHAMP during 10 March to 9 June through 2001–2005 are used.

[18] Figure 3 shows the local time coverage of the CHAMP observations for each day of 10 March to 9 June during each year. Observations in different years correspond to different local times, and the local time coverage shifts slowly by very few minutes a day. To provide the coverage over all local times needed, the data are combined for 2001–2005.

[19] Figure 4 gives the zonally averaged mean winds from CHAMP. These are the wind components in geographic coordinates (different from Figures 1a and 2a), but they are presented versus MLAT and MLT for which the wind measurements are taken. As the meridional wind components from CHAMP at low latitudes are not available, a transformation of the measurements into geomagnetic coordinates is not possible. The winds in magnetic conjugate hemispheres are binned. The plot shows that the largest wind velocity occurs at 21:00 MLT at low latitudes. The wind velocity is smaller in the early evening and at late night, and it decreases with increasing latitude. These features appear to be consistent with those seen in Figures 1a and 2a. Detailed comparison is presented in section 3 to demonstrate the relation of plasma depletion drifts with the background neutral winds and ion drifts.

3. Discussion

[20] The drift velocities of plasma depletions are shown in Figure 5 in comparison with the ambient ion drift velocities. The magnetic zonal components are presented as a function of local time in each plot. It is worth noting that the depletion drifts are measured at around 400 km altitude (where the O^+ airglow emission peaks) but the measurements of the ambient ion drifts are taken at ∼600 km altitude. The measurements at the same latitudes correspond to different apex altitudes between the depletion drifts and the ion drifts (see Figures 1 and 2). To remove this difference, the ion drift measurements are adjusted along a dipole magnetic field line. The velocities presented in the comparison are the adjusted values that correspond to the same apex altitudes between the ion drift and the depletion drift measurements.

[21] Figure 5 shows that in each plot the zonal drift velocities change with local time for both the depletion drifts and the ambient ion drifts. The depletion drift velocity is smaller than the ambient ion drift velocity at 1800–2000 MLT, and after 2000 their values are close to each other. The difference is large at 15° MLAT, and it is smaller at lower latitudes. This drift velocity difference should not be caused by the altitude difference of the measurements because the velocities shown in each plot have been adjusted for the same apex heights. Also, the latitudinal difference is not due to the impact of the magnetic field geometry as the drift velocities in terms of degrees/hour (included in the supporting information) have the same patterns.

[22] The zonal velocities of the depletion drifts and the ion drifts are shown versus MLAT in Figure 6 for 20:00–00:00 MLT. At each hour, the ambient ion drift velocities have almost the same values at different latitudes. The depletion drift velocities are similar to the ion drifts at 4°–10° MLAT, but the depletion drift velocities change sharply at higher latitudes. The zonal drift velocities of plasma depletions have a larger latitudinal gradient than the ambient ion drifts becoming significant at 12°–18° MLAT.

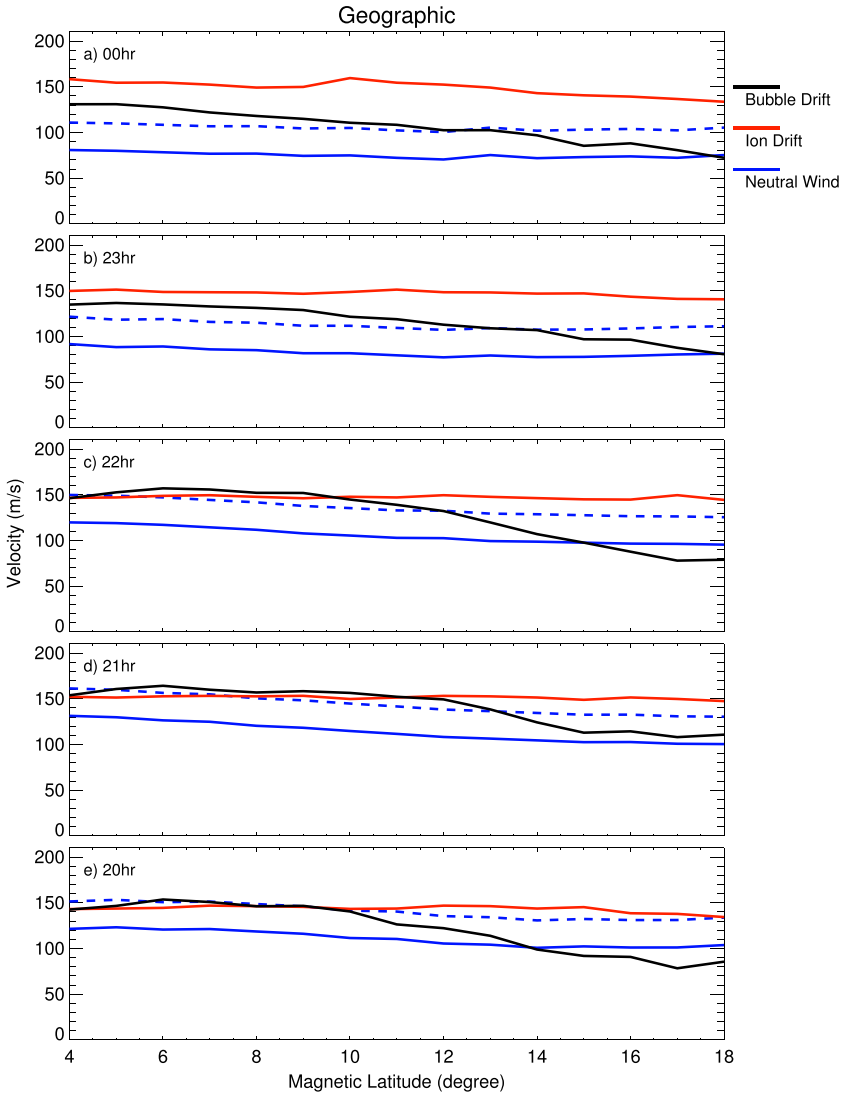

Figure 8. (a–e) Geographic zonal velocities of plasma depletion drifts (in black), ion drifts (in red), and neutral winds (in blue) at various MLTs, presented versus MLAT. The solid blue lines are for the measured neutral winds by CHAMP, and the dashed blue lines are for the adjusted neutral winds using the HWM93 model.

[23] This larger difference of higher latitudes is also noted above in Figure 5. As the ion drift velocities have been adjusted for the same apex altitudes as the depletion drift measurements, the difference seen here is not caused by the altitude difference of the measurements. The latitudinal difference is also not caused by the magnetic field geometry since the velocities presented in terms of degrees/hour have the same patterns (see supporting information).

[24] The CHAMP zonal winds are the components in the geographic zonal directions, but the plasma depletion drifts and the ion drifts are provided in magnetic coordinates. As the meridional wind components from CHAMP at low latitudes are not available, the transformation of the CHAMP winds into geomagnetic coordinates is not possible. The plasma depletion drifts and the ion drifts are transformed into the geographic zonal components to compare with the CHAMP zonal winds. Figures 1b and 2b present the transformed geographical zonal drift components. These components have similar variation patterns to the magnetic components as shown in Figures 1a and 2a.

[25] Figure 7 shows the geographic zonal velocities of the plasma depletion drifts in comparison with the ambient ion zonal drifts and the zonal neutral winds. The plasma depletions are observed during the year of 2002 while the neutral wind observations are combined from 2001 to 2005. As shown in Figure 3, the wind data during 2005 dominate. The average f10.7 solar flux value is 180 during 2002 but is only 90 for 2005. We have calculated the neutral wind velocities for 2002 and 2005 with the corresponding solar fluxes, using the HWM93 model [e.g., *Hedin*, 1992]. The neutral wind differences between 2002 and 2005 due to the solar flux change can be calculated. The mean difference is found to be about 30 m/s (about 1°/h). By adding the difference, the neutral winds are adjusted. The neutral winds adjusted for this difference are also included in the figure. The velocities included have also been adjusted for the same apex altitudes between different measurements (the plasma

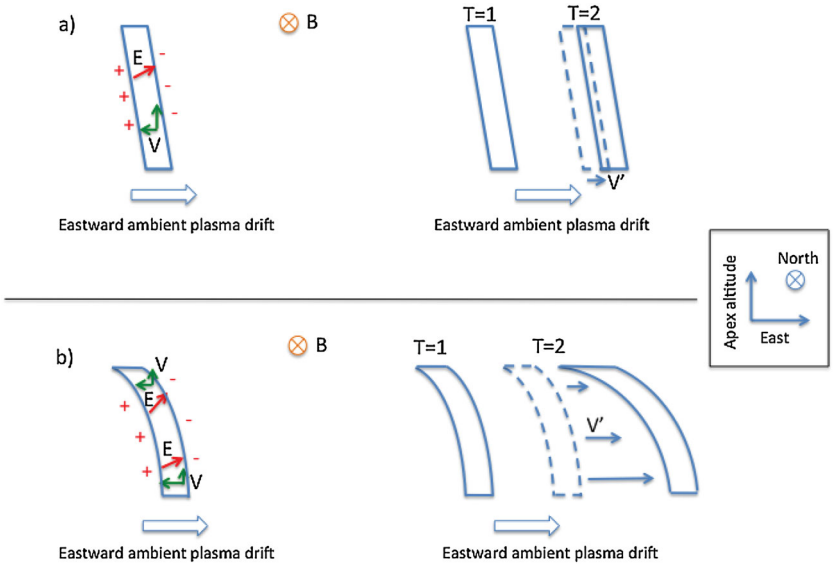

Figure 9. An illustration of plasma depletion drifts in relation to the ambient plasma drifts. (a) For the westward tilted plasma depletion, the zonal drifts of plasma inside the depletion structure (owing to $\mathbf{E} \times \mathbf{B}$) are westward with respect to the ambient plasma drifts. Consequently, the plasma builds up on the west wall of the structure and the depletion drifts to the east. (b) For the C-shaped (reversed C) plasma depletion, the zonal drifts of plasma inside the depletion are also westward and they change with increasing altitude (and latitude). The depletion drifts thus have a latitudinal gradient, being larger at higher latitudes.

depletion observations correspond to different apex altitudes from the ion drift measurements, but the depletion observations are for almost the same apex altitudes as the neutral wind observations; see Figures 1, 2, and 4).

[26] Figure 7 shows a similar pattern between different plots. In each plot, the depletion drift velocities are smaller than both the ion drift velocities and the neutral winds at 18:00–20:00 MLT, and after 21:00, the variations of these velocities are rather similar. The velocity difference at 18:00–20:00 MLT increases with increasing latitude, and it is smaller at lower latitudes.

[27] The difference of the plasma depletion drifts with the background neutral winds has been discussed in previous studies [e.g., *Chapagain et al.*, 2012, 2013]. The results shown here confirm that the plasma depletions do not simply drift with the background specifically at 18:00–20:00 MLT in the early evening when the *E* region dynamo is still present. The studies by *Chapagain et al.* [2012, 2013] have also shown that the depletion drift velocities are approximately equal to the neutral wind speeds at nighttime hours after 22:00. This study finds that the difference of the plasma depletion drifts with the background winds is smaller at lower latitudes. This explains the previous observations from single locations near the equator.

[28] The latitudinal variation of the plasma depletion drifts is compared with the variations of the simultaneously observed ion drifts and neutral winds in Figure 8 for the local times of 20:00–00:00. The common feature is that at 12°–18° MLAT, the depletion drift velocities have a larger gradient than the ion drift velocities and the neutral winds. This latitudinal gradient difference has been reported by *Huba et al.* [2009] and *England and Immel* [2012] using the model studies. This study compares the satellite observations and compares the depletion drifts with both the neutral winds and the ambient plasma drifts. The study shows that the latitudinal gradient in the plasma depletion drifts differ from the ambient plasma drifts as well as the neutral winds. The study provides a measure of the latitudinal difference from a global perspective.

[29] It has been previously suggested that polarization electric fields inside the plasma depletions are responsible for the eastward drift of the depletion structures [e.g., *Huang et al.*, 2010]. As proposed by *England and Immel* [2012], the polarization electric fields could also explain the latitudinal gradient in plasma depletion drift velocities observed here in this study.

[30] Figure 9a (as proposed by *Huang et al.* [2010]) illustrates that for the westward tilt depletion, the zonal drift velocity of plasma inside the depletion structure is westward, owing to the polarization electric fields. For this, the plasma builds up on the westward wall of the depletion structure and the depletion structure moves to the east. Extending the theory proposed by *Huang et al.* [2010], Figure 9b illustrates that for the C-shaped (reversed C) depletion, the polarization electric fields also drive a westward drift of plasma inside the depletion and the drift changes with increasing latitude. The result is that the plasma depletion drifts have a latitudinal gradient becoming larger at higher latitudes.

[31] It is worth noting that the comparison of the plasma depletion drifts and ion drifts with the background neutral winds presented in this study is at a single altitude. Specifically, the wind observations used in this comparison shows only one piece of the neutral wind contribution to the overall electrodynamics of the nighttime equatorial ionosphere, which is a flux-tube-integrated effect. However, our study is useful for understanding the motion of plasma

depletions and the ion-neutral coupling because the *F* region wind dynamo dominates the zonal plasma drifts during the nighttime [e.g., *Heelis*, 2004] and the vertical gradient in the winds at *F* region altitudes is believed to be small [e.g., *Heelis*, 2004; *Shepherd et al.*, 2012]. Thus, the impact of not including wind observations from different altitudes is believed to be limited.

4. Conclusions

[32] This study analyzes the zonal drift velocities of the O^+ plasma depletions at 350–400 km altitude in the post sunset equatorial ionosphere as observed by the IMAGE satellite during the time period of 10 March to 7 June 2002. These velocities are compared with the ambient ion drift velocities measured simultaneously by the ROCSAT-1 satellite for the same time period. The plasma depletion drifts are also compared with the thermospheric neutral winds at ∼400 km altitude measured by the CHAMP satellite for the similar time period. These simultaneous and global-scale satellite observations allow for an examination of the local time and latitude variations of the plasma depletion drifts and provide a comparison between the depletion drifts and the background neutral winds as well as the plasma drifts.

[33] The analysis shows that the zonal drift velocity of plasma depletions is smaller than both the ambient ion drift velocity and the neutral wind at 18:00–20:00 MLT, and after, 21:00 the variations of these velocities are similar. The analysis also shows that the difference of the depletion drifts with the background is smaller at lower latitudes. This is the first-ever satellite comparison of the plasma depletion drift with the ambient plasma drift as well as the neutral wind for a global scale, explaining many previous observations at a single location.

[34] Furthermore, the study finds that the plasma depletion drift velocities have a large latitudinal gradient at 12°–18° magnetic latitude, which again does not match the ambient ion drifts and the neutral winds. This latitudinal difference has been reported by previous studies, but those studies use models and they only compare the depletion drifts with the modeled neutral winds. This study compares the satellite observations and compares with both the neutral winds and the plasma drifts. The study provides a measure of the difference that has never been studied by any study using global observations.

[35] The latitudinal gradient in the zonal drift velocity of plasma depletions could be due to polarization electric fields generated inside the depletion structures [e.g., *Huang et al.*, 2010]. For the C-shaped plasma depletion, the polarization electric fields drive a westward drift of plasma inside the depletion and this drift changes with increasing latitude. The consequence would be that the depletion drifts have a latitudinal gradient becoming significant at higher latitudes.

[36] **Acknowledgments.** This research work was supported by NASA's Living With a Star program through award NNX11AP04G. We acknowledge NASA for contract NAS5-02099 and NSF for support of GIMNAST through grant AGS-1004736. The National Center for Atmospheric Research is supported by the National Science Foundation. The ROCSAT-1 ion drift velocity data are available at csrsddc.csrsr.ncu.edu.tw. The authors thank Shin-Yi Su at National Central University for the assistance with the ROCSAT-1 data.

[37] Robert Lysak thanks Vince Eccles and an anonymous reviewer for their assistance in evaluating this paper.

References

Abdu, M. A., I. S. Batista, J. H. A. Sobral, E. R. de Paula, and I. J. Kantor (1985), Equatorial ionospheric plasma bubble irregularity occurrence and zonal velocities under quiet and disturbed conditions, from polarimeter observations, *J. Geophys. Res.*, *90*, 9921–9928, doi:10.1029/JA090iA10p09921.

Anderson, D. N., and M. Mendillo (1983), Ionospheric conditions affecting the evolution of equatorial plasma depletions, *Geophys. Res. Lett.*, *10*, 541–544.

Basu, S., K. M. Groves, S. Basu, and P. J. Sultan (2002), Specification and forecasting of scintillations in communication/navigation links: Current status and future plans, *J. Atmos. Sol. Terr. Phys.*, *64*, 1745–1754, doi:10.1016/S1364-6826(02)00124-4.

Chapagain, N. P., J. J. Makela, J. W. Meriwether, D. J. Fisher, R. A. Buriti, and A. F. Medeiros (2012), Comparison of nighttime zonal neutral winds and equatorial plasma bubble drift velocities over Brazil, *J. Geophys. Res.*, *117*, A06309, doi:10.1029/2012JA017620.

Chapagain, N. P., D. J. Fisher, J. W. Meriwether, J. L. Chau, and J. J. Makela (2013), Comparison of zonal neutral winds with equatorial plasma bubble and plasma drift velocities, *J. Geophys. Res. Space Physics*, *118*, 1802–1812, doi:10.1002/jgra.50238.

Coley, W. R., and R. A. Heelis (1989), Low-latitude zonal and vertical ion drifts seen by DE 2, *J. Geophys. Res.*, *94*, 6751–6761, doi:10.1029/JA094iA06p06751.

Doornbos, E., et al. (2010), Neutral density and crosswind determination from arbitrarily oriented multiaxis accelerometers on satellites, *J. Spacecraft Rockets*, *47*, 580–589, doi:10.2514/1.48114.

England, S. L., and T. J. Immel (2012), An empirical model of the drift velocity of equatorial plasma depletions, *J. Geophys. Res.*, *117*, A12308, doi:10.1029/2012JA018091.

Fejer, B. G., S. A. Gonzalez, E. R. de Paula, and R. F. Woodman (1991), Average vertical and zonal F region plasma drifts over Jicamarca, *J. Geophys. Res.*, *96*, 13,901–13,906.

Fejer, B. G., L. Scherliess, and E. R. de Paula (1999), Effects of the vertical plasma drift velocity on the generation and evolution of equatorial spread F, *J. Geophys. Res.*, *104*, 19,859–19,870, doi:10.1029/1999JA900271.

Haase, J. S., T. Dautermann, M. J. Taylor, N. Chapagain, E. Calais, and D. Pautet (2011), Propagation of plasma bubbles observed in Brazil from GPS and airglow data, *Adv. Space Res.*, *47*, 1758–1776, doi:10.1016/j.asr.2010.09.025.

Hedin, A. E. (1992), MSISE model (1990), *Planet. Space Sci.*, *40*, 556–556, doi:10.1016/0032-0633(92)90210-F.

Heelis, R. A. (2004), Electrodynamics in the low and middle latitude ionosphere: A tutorial, *J. Atmos. Sol. Terr. Phys.*, *66*, 825–838, doi:10.1016/j.jastp.2004.01.034.

Huang, C.-S., and M. C. Kelley (1996), Nonlinear evolution of equatorial spread F: 1. On the role of plasma instabilities and spatial resonance associated with gravity wave seeding, *J. Geophys. Res.*, *101*, 283–292, doi:10.1029/95JA02211.

Huang, C.-S., O. de La BeaujardièRe, R. F. Pfaff, J. M. Retterer, P. A. Roddy, D. E. Hunton, Y.-J. Su, S.-Y. Su, and F. J. Rich (2010), Zonal drift of plasma particles inside equatorial plasma bubbles and its relation to the zonal drift of the bubble structure, *J. Geophys. Res.*, *115*, A07316, doi:10.1029/2010JA015324.

Huang, C.-S., O. de La BeaujardièRe, P. A. Roddy, D. E. Hunton, J. O. Ballenthin, M. R. Hairston, and R. F. Pfaff (2013), Large-scale quasiperiodic plasma bubbles: C/NOFS observations and causal mechanism, *J. Geophys. Res. Space Physics*, *118*, 3602–3612, doi:10.1002/jgra.50338.

Huba, J. D., G. Joyce, and J. Krall (2008), Three-dimensional equatorial spread F modeling, *Geophys. Res. Lett.*, *35*, L10102, doi:10.1029/2008GL033509.

Huba, J. D., S. L. Ossakow, G. Joyce, J. Krall, and S. L. England (2009), Three-dimensional equatorial spread F modeling: Zonal neutral wind effects, *Geophys. Res. Lett.*, *36*, L19106, doi:10.1029/2009GL040284.

Immel, T. J., S. B. Mende, H. U. Frey, L. M. Peticolas, and E. Sagawa (2003), Determination of low latitude plasma drift speeds from FUV images, *Geophys. Res. Lett.*, *30*(18), 7–1, doi:10.1029/2003GL017573.

Kelley, M. C., M. F. Larsen, C. La Hoz, and J. P. McClure (1981), Gravity wave initiation of equatorial spread F: A case study, *J. Geophys. Res.*, *86*, 9087–9100, doi:10.1029/JA086iA11p09087.

Kil, H., and R. A. Heelis (1998), Global distribution of density irregularities in the equatorial ionosphere, *J. Geophys. Res.*, *103*, 407–418, doi:10.1029/97JA02698.

Lieberman, R. S., R. A. Akmaev, T. J. Fuller-Rowell, and E. Doornbos (2013), Thermospheric zonal mean winds and tides revealed by CHAMP, *Geophys. Res. Lett.*, *40*, 2439–2443, doi:10.1002/grl.50481.

Lin, C. S., T. J. Immel, H.-C. Yeh, S. B. Mende, and J. L. Burch (2005), Simultaneous observations of equatorial plasma depletion by

IMAGE and ROCSAT-1 satellites, *J. Geophys. Res.*, *110*, A06304, doi:10.1029/2004JA010774.

Makela, J. J. (2006), A review of imaging low-latitude ionospheric irregularity processes, *J. Atmos. Sol. Terr. Phys.*, *68*, 1441–1458, doi:10.1016/j.jastp.2005.04.014.

Martinis, C., J. V. Eccles, J. Baumgardner, J. Manzano, and M. Mendillo (2003), Latitude dependence of zonal plasma drifts obtained from dual-site airglow observations, *J. Geophys. Res.*, *108*(A3), 1129, doi:10.1029/2002JA009462.

Mendillo, M., and A. Tyler (1983), Geometry of depleted plasma regions in the equatorial ionosphere, *J. Geophys. Res.*, *88*, 5778–5782.

Pacheco, E. E., R. A. Heelis, and S.-Y. Su (2010), Quiet time meridional (vertical) ion drifts at low and middle latitudes observed by ROCSAT-1, *J. Geophys. Res.*, *115*, A09308, doi:10.1029/2009JA015108.

Park, S. H., S. L. England, T. J. Immel, H. U. Frey, and S. B. Mende (2007), A method for determining the drift velocity of plasma depletions in the equatorial ionosphere using far-ultraviolet spacecraft observations, *J. Geophys. Res.*, *112*, A11314, doi:10.1029/2007JA012327.

Retterer, J. M. (2010), Forecasting low-latitude radio scintillation with 3-D ionospheric plume models: 1. Plume model, *J. Geophys. Res.*, *115*, A03306, doi:10.1029/2008JA013839.

Shepherd, G. G., et al. (2012), The Wind Imaging Interferometer (WINDII) on the Upper Atmosphere Research Satellite: A 20 year perspective, *Rev. Geophys.*, *50*, RG2007, doi:10.1029/2012RG000390.

Su, S.-Y., H. C. Yeh, and R. A. Heelis (2001), ROCSAT 1 ionospheric plasma and electrodynamics instrument observations of equatorial spread F: An early transitional scale result, *J. Geophys. Res.*, *106*, 29,153–29,160, doi:10.1029/2001JA900109.

Su, S.-Y., C. H. Liu, H. H. Ho, and C. K. Chao (2006), Distribution characteristics of topside ionospheric density irregularities: Equatorial versus midlatitude regions, *J. Geophys. Res.*, *111*, A06305, doi:10.1029/2005JA011330.

Su, S.-Y., C. K. Chao, and C. H. Liu (2009), Cause of different local time distribution in the postsunset equatorial ionospheric irregularity occurrences between June and December solstices, *J. Geophys. Res.*, *114*, A04321, doi:10.1029/2008JA013858.

Tsunoda, R. T., R. C. Livingston, J. P. McClure, and W. B. Hanson (1982), Equatorial plasma bubbles: Vertically elongated wedges from the bottomside F layer, *J. Geophys. Res.*, *87*, 9171–9180, doi:10.1029/JA087iA11p09171.

Valladares, C. E., R. Sheehan, S. Basu, H. Kuenzler, and J. Espinoza (1996), The multi-instrumented studies of equatorial thermosphere aeronomy scintillation system: Climatology of zonal drifts, *J. Geophys. Res.*, *101*, 26,839–26,850, doi:10.1029/96JA00183.

Zalesak, S. T., S. L. Ossakow, and P. K. Chaturvedi (1982), Nonlinear equatorial spread F: The effect of neutral winds and background Pedersen conductivity, *J. Geophys. Res.*, *87*, 151–166.